Numerical Modelling of Hydraulic Efficiency and Pollution Transport in Waste Stabilization Ponds

Danial Goodarzi [a], Abdolmajid Mohammadian [a], Jonathan Pearson [b], Soroush Abolfathi [b,*]

[a] *Department of Civil Engineering, University of Ottawa, 75 Laurier Ave E, Ottawa, ON, K1N 6N5, Canada*

[b] *School of Engineering, The University of Warwick, CV4 7AL, Coventry, United Kingdom*

Abstract

This paper investigates the hydraulic performance and solute transport processes in waste stabilization ponds (WSPs). A numerical model comprised of Reynolds-averaged Navier–Stokes (RANS) flow hydrodynamic model with the standard $k-\varepsilon$ turbulence closure coupled with the advection-diffusion solute transport model, is developed in a three-dimensional Cartesian coordinate system. The proposed numerical model is successfully validated against laboratory-scale physical modelling measurements of flow hydrodynamics and solute characteristics across trapezoidal pond geometry. The developed numerical model is adopted to run series of scenario-based simulations to investigate the effects of WSP's geometrical features and implementation of an island retrofitting on the hydraulic performance and treatment efficiency of the WSPs . Fifteen pond configurations with varying side-walls slope and island configurations are simulated. Vertical and

* Corresponding author: Soroush.Abolfathi@warwick.ac.uk

horizontal structures of flow hydrodynamics across the pond are investigated. Solute transport processes are studied through determining residence time distribution (RTDs) curves based on numerical tracer simulations. Two deflector island configurations (parallel and rotated) are simulated to investigate their influence on enhancing the hydraulic performance of the WSP. The analysis of the numerical results indicates an overall positive impact of deflector island retrofitting on the hydraulic performance of the WSP. The side-walls slope are shown to play a key role in determining the overall performance of the WSP. For the cases with side-walls slope of 1:1, 0.5:1 and 0:1, the hydraulic efficiency of the WSP was enhanced by adding both parallel and rotated islands. However, for the cases with side-walls slope of 2:1 and 1.5:1, addition of island deflector is shown to have negative impacts on the hydraulic performance of the waste stabilization pond.

Keywords: RANS; hydrodynamics; waste stabilization pond (WSP); residence time; pollution transport; mixing

1. Introduction

The world population growth, anthropogenic activities induced by domestic and agriculture and industrial developments, increase stress on both quantity and quality of water resources. Efficient and effective treatment of water and wastewater using sustainable low-emission methods is one of the key priorities for water resource management around the world [1-6]. Complying with tightening environmental, energy efficiency and public health standards is a challenging task for the water industry and of particular importance for sustainable water resource management [7, 8]. The long-term

impacts of climate change and the vital necessity to reduce emissions highlights the need for transitioning towards more sustainable low-emission water and wastewater treatment technologies. Therefore, there is an ever-increasing demand to enhance the efficiency, improve the design and operational protocols of water and wastewater treatment processes to cope with the increasing pressure and demand in terms of water quality and environmental protection standards [9-11].

Large treatment ponds such as waste stabilization ponds (WSPs) are simple to design, cost-effective and flexible in operation and maintenance processes. One of the most important benefits of adopting these treatment ponds as a part of the treatment process is their tolerance towards system shocks and large fluctuations in wastewater characteristics, including flow rate, biochemical oxygen demand, total suspended solids and ambient and inflow temperature. The waste stabilization ponds (WSPs) are capable of providing an appropriate level of treatment for wastewater from urban, agriculture and food industry [12, 13]. Hydraulic characteristics of WSPs, such as effective volume, hydraulic retention time and short-circuiting, can heavily influence the interactions of micro-organism with wastewater, and the consequent pollution removal and treatment efficiency [14, 15]. A detailed understanding of WSP's hydraulic performance is essential to ensure appropriate and efficient design to safeguard public health and the environment.

Plug-flow regime in many physical, chemical and biological treatment processes of water and wastewater is an ideal hydraulic condition leading to maximum efficiency of the mixing and treatment process. In plug-flow condition, all the control volume of the water

entering the pond have the same hydraulic retention time (HRT), which is equal to the nominal hydraulic retention time (HRT_N) described by Eq. 1:

$$HRT_N = \frac{V}{Q} \quad (1)$$

where V is volume of the system [m^3] and Q represents the inflow rate [$m^3.s^{-1}$]. In real-life conditions, idealized plug flow regime doesn't occur and therefore a mismatch between HRT and HRT_N often exits. Climate conditions such as the effects of wind, thermal stratification, sunlight, and extreme events (e.g., intense precipitations or prolong drought) can play an important role in altering flow conditions and treatment efficiency of WSPs. Furthermore, geometrical properties of WSPs including inlet, outlet and baffle orientations, as well as operational conditions (e.g., sludge accumulation) can adversely impact the hydraulic efficiency of WSPs by allowing short-circuiting, dead zones, and reducing the effective volume [16-21].

The majority of existing studies on the performance of WSPs have focused on physical models with tracer tests and drogue tracking technologies to examine the effects of flow hydrodynamic on the mixing and transport of solute across the ponds. However, tracer studies and drogue tracking techniques are limited to concentration data at the outlet and the horizontal two-dimensional velocity profiles inside the pond, respectively [22-28]. The results from field-based measurements are likely to have uncertainties due to measurement inaccuracy and challenges associated with the calibration of fluorometric and velocimetry devices, exacerbated by adverse climatic effects (e.g., wind effects, thermal stratifications due to sunlight) on the hydrodynamic of the WSPs.

Previous studies investigated the optimum hydrodynamic regime in WSPs to allow maximum retention time and complete mixing for effective treatment of solute within the pond [29-32]. Reduced-order models including completely mixed flow, ponds-in-series and dispersion models are amongst the methods proposed for predictions of hydraulics characteristics in WSPs [29-32]. However, the existing models are not capable of accurate prediction of the effects of geometrical configurations on hydraulics characteristics and detailed spatiotemporal varying flow hydrodynamics structures within the WSPs, leading to large uncertainties in their predictions of WSP's key performance characteristics including residence time distribution (RTD), dead zones and short-circuiting.

Early applications of computational fluid dynamics (CFD) in study of waste stabilization ponds was conducted by Wood et al. [33, 34]. They investigated the effects of WSP design configurations on the hydraulic performance of a large rectangular pond and showed the impacts of the location and geometrical properties of inlet and outlet location on the flow pattern and hydrodynamics structure across the pond. Presson [17] proposed a two-dimensional numerical model to examine the effects of geometrical setups for baffles and inlet/outlet location on the hydraulic behavior of large ponds [17]. The significance of inlet and outlet configurations on the hydraulic efficiency of ponds is highlighted in several studies [14, 30, 31, 32]. The hydraulic performance of engineered treatment ponds with diagonal inlet and outlet locations were reported to be similar to those with the directly facing inlet/outlet locations [17, 35]. Several studies highlighted that the hydraulic efficiency of ponds improves by increasing the distance between inlet

and outlet. This is due to the extended flow path between inlet and outlet boundaries, facilitating an enhanced mixing and dilution of solute in the treatment pond [17, 36-38]. Implementation of baffle structures was shown to have significant effects on improving the hydraulic efficiency in long ponds by increasing the flow transport time across the pond [16, 39, 40]. Determining an appropriate design and configuration for transverse and longitudinal baffles can reduce flow short-circuiting, increase the hydraulic retention time (HRT), and treatment efficiency of the treatment ponds [35, 41-44]. Measurements from a range of field-based and physical modelling studies show that measures such as distributed vegetation and floating treatment wetlands can further enhance the hydraulic performance and treatment efficiencies in WSPs [45-47].

Retrofitting of deflector islands is an effective measure for improving treatment efficiency of WSPs. However, the optimum geometry and orientation of deflector islands, and their role on influencing the hydrodynamics and solute mixing processes within WSPs is not fully understood. Khan et al. [48] investigated large treatment ponds and reported detrimental effects of deflector islands on short-circuiting condition within the pond. They hypothesized that the poor hydraulic efficiency of the pond with deflector island can be associated with the geometrical configurations of the pond including the side-walls slope. Given that inappropriate hydraulic conditions in treatment ponds can drastically reduce the efficiency of the ponds and increases the operational and maintenance costs, understanding the flow hydrodynamics and the effects of geometrical properties of ponds on the underlying transport and mixing processes is vital to ensure appropriate design and operational protocols for more widespread adoption of natural capitals into water and wastewater treatment strategies.

Flow and solute interactions with WSP's geometry can generate complex hydrodynamic processes across the pond which can be influenced by a range of design, operational and climatic factors. Hence, rigorous multi-component investigations are needed for optimal hydraulic design of waste stabilization ponds [49]. This paper develops a robust and computationally affordable numerical modelling framework which incorporates RANS hydrodynamic model with the standard $k-\varepsilon$ turbulence closure and advection-diffusion solute transport model, to simulate the effects of geometrical properties and retrofitting solutions on the hydraulic performance and solute mixing in WSPs.

2. Mathematical modelling

2.1. Flow hydrodynamics model and governing equations

In this study a three-dimensional hydrodynamic model governed by single-phase RANS equations is developed [50]. The conservation of mass and momentum are defined by time averaged continuity (Eq.2) and Navier-Stokes (Eq.3) equations:

$$\frac{\partial \bar{v}_i}{\partial x_i} = 0 \tag{2}$$

$$\rho \frac{\partial \bar{v}_i}{\partial t} + \rho \frac{\partial \bar{v}_i \bar{v}_j}{\partial x_j} = -\frac{\partial \bar{p}}{\partial x_i} + \frac{\partial}{\partial x_j}\left(\mu \frac{\partial \bar{v}_i}{\partial x_j} - \rho \overline{v_i' v_j'} \right) \tag{3}$$

where ρ denotes density [kg/m^3], v is velocity [m/s], t denotes time [s], p is the hydrodynamic pressure [kg/m.s^2], μ is dynamic viscosity [kg/m.s] and $\overline{v_i' v_j'}$ is Reynolds

stress tensor. Finite-volume numerical method was adopted for discretizing the governing equations of fluid motion and solute transport in the WSP [51].

Flow turbulence and eddy viscosity in RANS equations are computed using the standard $k-\varepsilon$ turbulence closure model described by Jones and Launder [52]. The reliability and numerical stability of the $k-\varepsilon$ model used in this paper has been demonstrated in several related numerical studies [e.g., 20, 33, 49, 53, 54]. Turbulent viscosity μ_t is derived based on Boussinesq hypothesis as:

$$\nu_t = C_\mu \frac{k^2}{\varepsilon} \tag{4}$$

where the turbulent kinetic energy k [m^2/s^2] and the turbulent energy dissipation rate ε [m^2/s^3] are determined using the numerical procedures described by Eq.5 and 6, as follow:

$$\frac{\partial k}{\partial t} + \bar{v}_j \frac{\partial k}{\partial x_j} = \nu_t \left(\frac{\partial \bar{v}_i}{\partial x_j} + \frac{\partial \bar{v}_j}{\partial x_i} \right) \frac{\partial \bar{v}_i}{\partial x_j} - \varepsilon + \frac{\partial}{\partial x_j} \left[\left(\nu + \frac{\nu_t}{\sigma_k} \right) \frac{\partial k}{\partial x_j} \right] \tag{5}$$

$$\frac{\partial \varepsilon}{\partial t} + \bar{v}_j \frac{\partial \varepsilon}{\partial x_j} = \frac{\varepsilon}{k} C_{\varepsilon 1} \nu_t \left(\frac{\partial \bar{v}_i}{\partial x_j} + \frac{\partial \bar{v}_j}{\partial x_i} \right) \frac{\partial \bar{v}_i}{\partial x_j} - C_{\varepsilon 2} \frac{\varepsilon^2}{k} + \frac{\partial}{\partial x_j} \left[\left(\nu + \frac{\nu_t}{\sigma_\varepsilon} \right) \frac{\partial \varepsilon}{\partial x_j} \right] \tag{6}$$

where ν_t is kinematic turbulent viscosity [m^2/s]. Table 1 summarizes the numerical constant used in this study for the development of turbulence closure model [50]. The numerical constants described in Table 1 are adopted to ensure the numerical model can

replicate appropriate flow characteristics similar to the flow regime in a typical WPS setting.

Table 1- Numerical constants for the *k-ε* turbulence closure model

Numerical constant	Value
$C_{\varepsilon 1}$	1.44
$C_{\varepsilon 2}$	1.92
C_{μ}	0.09
σ_k	1
σ_{ε}	1.3

2.2. Solute Transport Modelling

Ideal flow regime assumption with plug flow and complete mixing is widely used for the design and operation of water and wastewater treatment ponds [19]. In plug flow regime, the fluid flows into the domain equally distributed with no longitudinal mixing and similar flow velocity profiles across the pond domain (e.g., rectangular sedimentation tanks). In complete mixing condition, the fluid properties can be considered as well-mixed and homogeneous at any spatial location and time instance (e.g., activated sludge reactor). Hydraulic efficiency of operating water and wastewater treatment ponds is usually lower than their designed stage which can lead to treatment inefficiency and consequent pollution discharge into the environment. Hence, it is essential to maximize the hydraulic efficiency of treatment ponds by increasing the pollution removal capacity and reduction in process costs. Understanding flow hydrodynamic and transport patterns under different design configurations is key for evaluating hydraulic efficiency of WSPs and design optimization processes. Analysis of residence time distributions (RTD) from tracer data provides comprehensive insight into pollution transport and mixing patterns in ponds.

RTD curves are obtained from instantaneous injection of a non-reactive passive scalar at inlet of the pond and temporal measurement of scalar concentration at the outlet [55].

Non-reactive passive scalar tracer transport is simulated in this study by implementing advection-diffusion equation (Eq.7), resolved in three-dimensional Cartesian coordinates system. The tracer transport and RANS hydrodynamic models are computed simultaneously at each numerical time-step [56].

$$\frac{\partial \bar{C}}{\partial t} + v_i \frac{\partial \bar{C}}{\partial x_j} = \frac{\partial}{\partial x_i}\left[(D + D_t)\frac{\partial \bar{C}}{\partial x_i}\right] \quad (7)$$

where C is tracer concentration [unit: mass/m^3], D and D_t represent molecular diffusion coefficient and turbulent molecular diffusion coefficient [m^2/s], respectively. The turbulent Schmidt number is taken as one for all simulation scenarios ($Sc_T = 1$) [non-dimensional] [57].

To facilitate comparison and interpretation of retention time distribution (RTD) for different simulation scenarios, the RTDs are normalized by dividing the numerically measured concentration (C) at the outlet to the average concentration injected in the inlet boundary divided by the pond volume (C_0).

$$C(\theta) = \frac{C}{C_0} \quad (8)$$

Normalized time θ, is defined according to Eq. 9:

$$\theta = \frac{t}{T} \tag{9}$$

where, T is theoretical retention time [s].

The real hydraulic retention time (HRT_R) and hydraulic efficiency (λ) of the pond are determined based on averaged temporal variations of tracer concentration at the outlet [2, 11, 39]:

$$HRT_R = \frac{\int_0^\infty tc(t)dt}{\int_0^\infty c(t)dt} \tag{10}$$

$$\lambda = \frac{T_{peak}}{HRT_N} \tag{11}$$

Effective volume of the pond *e*, is determined as the ratio of real hydraulic retention to nominal hydraulic retention time (Eq.12):

$$e = \frac{HRT_R}{HRT_N} \tag{12}$$

Short-circuit is a condition caused by rapid transport and advection of the solute inside the pond. Short-circuit usually occurs when the fluid transport from the inlet to the outlet of the domain in a direct path, without desirable level of mixing and earlier than the theoretical retention time (*T*). The short-circuiting index S_I is determined in this study using

$$S_I = \frac{t_i}{HRT_R} \quad (13)$$

where t_i denotes the time duration that tracer reaches the outlet.

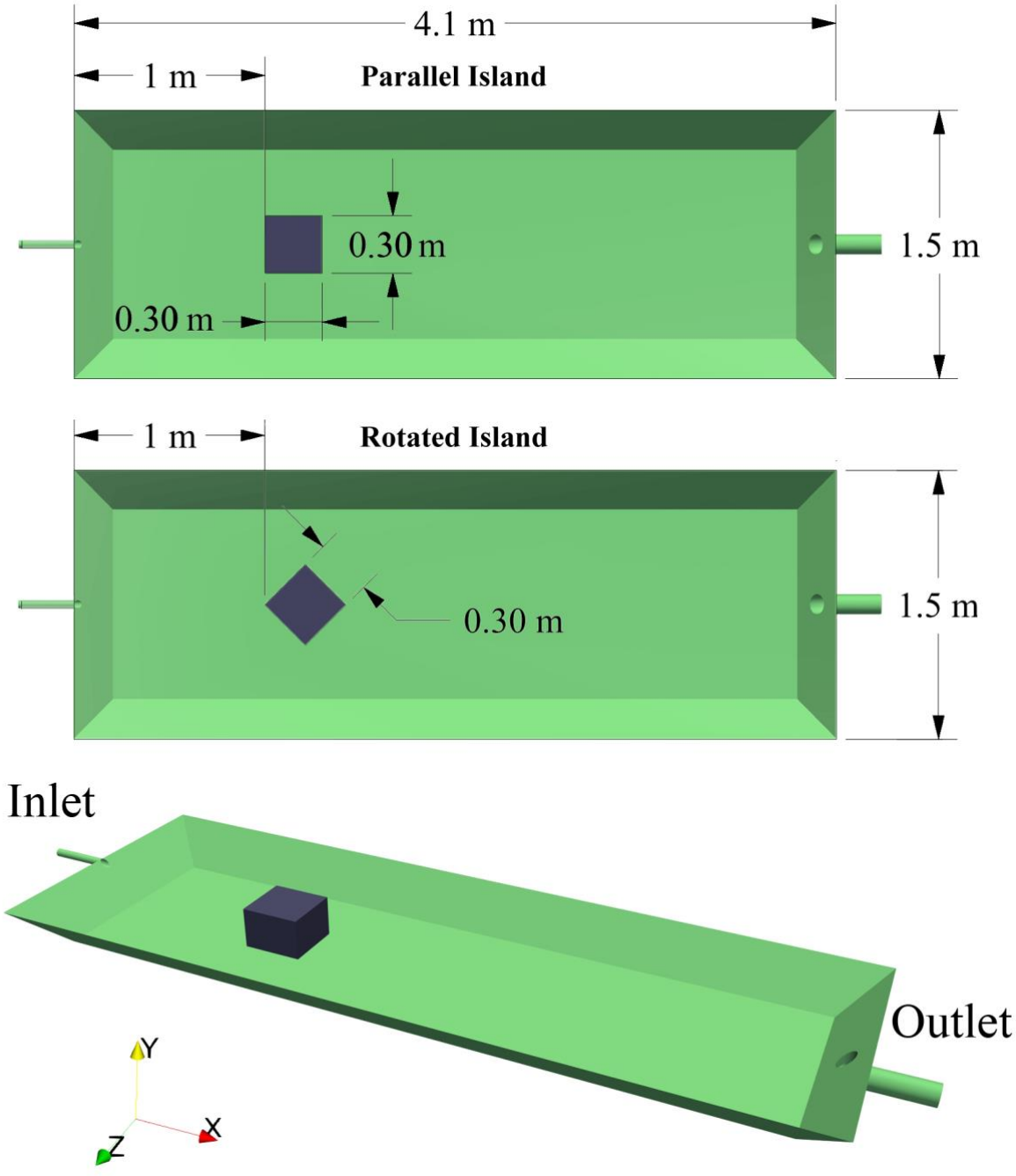

Figure 1- Geometrical properties of the waste stabilization pond and island orientations

2.3. Computational domain

The numerical model described and developed in §2.1. and §2.2. is adopted to simulate flow hydrodynamics and solute transport processes in a three-dimensional scaled trapezoidal pond. The pond modelled in this study has dimension of 4.1m (L) × 1.5m (W) × 0.23m (H) with a bank slope of 2:1 (*v*:*h*). The geometrical properties of the pond are defined following Khan et al. [43] detailed physical modelling study of solute transport in treatment pond. The inlet boundary is a pipe with 42mm diameter which is located horizontally at the center of the front wall of the pond and below the water surface. The outlet boundary is a pipe with a diameter of 105mm located at the center of the opposite end of the pond (see Figure. 1).

The hydraulic efficiency of the waste stabilization pond with two commonly used impermeable island orientations and a range of bank slopes (= 2:1, 1.5:1, 1:1, 0.5:1, and 0:1) was examined using the numerical model described in §2.1 and §2.2. The square island is located at 1m from the inlet boundary which is equal to one quarter of the pond length. Two island configurations, with 90- and 45-degrees' orientations with the pond walls are tested in this study to quantify the influence of island orientations on the performance of waste stabilization ponds (WSPs). Figures 1 and 2 illustrate schematic of the WSP, island configurations and side-walls slope investigated in this study.

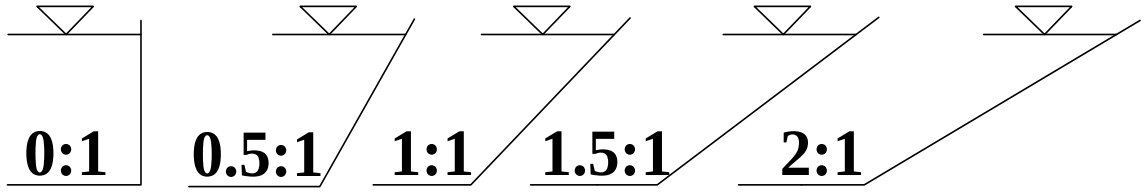

Figure 2 - Schematic of different side-walls slopes

Table 2 presents summary of the 15 numerical scenarios and geometrical configurations investigated in this study. In order to recall each simulation case easily, the simulation scenarios are named based on of island orientation followed by side-walls slope of the pond (see 'case name' in Table 2). The first two letters of the case name indicate the island configuration followed by the side-walls slope of the pond. The geometrical and retrofitting details of the scenarios proposed in Table 2 are considered following the most common design protocols for WSPs, and to ensure that a comprehensive range of widely-used configurations are analyzed in this study.

The numerical model developed in this study was implemented using Open-source Field Operation And Manipulation (OpenFOAM) model. The inlet boundary was modelled using mapped boundary condition to ensure fully developed flow regime can be reached at the inlet of the pond and avoid effects of pre-defined turbulence parameters in $k-\varepsilon$ model. An average flow rate of 0.001m^3/s was introduced at the inlet for all the test cases. The water elevation is kept constant at 0.23m for the duration of numerical simulations and across all scenarios.

Table 2 – Summary of simulation scenarios across all the test cases

Case	Length (m)	Width (m)	Depth (m)	Island type	Bank slope	Case name
1				No Island	2:1	NI_2-1
2				No Island	1.5:1	NI_1.5-1
3				No Island	1:1	NI_1-1
4				No Island	0.5:1	NI_0.5-1
5				No Island	0:1	NI_0-1
6				Parallel Island	2:1	PI_2-1
7				Parallel Island	1.5:1	PI_1.5-1
8	4.1	1.5	0.23	Parallel Island	1:1	PI_1-1
9				Parallel Island	0.5:1	PI_0.5-1
10				Parallel Island	0:1	PI_0-1
11				Rotated Island	2:1	RI_2-1
12				Rotated Island	1.5:1	RI_1.5-1
13				Rotated Island	1:1	RI_1-1
14				Rotated Island	0.5:1	RI_0.5-1
15				Rotated Island	0:1	RI_0-1

Given the nature of fluid flow in waste stabilization pond, the effects of free-surface generated turbulence are negligible. Therefore, in order to optimize the computational costs, free-surface effects are not computed during the simulations and, a symmetry boundary condition was implemented at the top boundary of the numerical domain to mimic no shear resistance at the surface of water as well as no water/scalar exchange through the boundary. Specified pressure and no-slip boundary conditions were set for outlet and walls, respectively. The boundary conditions were chosen to achieve robust computational algorithm, high-accuracy results and optimized computational costs. Further details of the boundary conditions used for this study are given in Table 3.

Table 3 – Boundary conditions adopted for flow hydrodynamic and solute transport variables

Flow variable	Boundary conditions			
	Inlet	**Outlet**	**Top**	**Side walls and bottom**
Velocity	mapped	inletOutlet	symmetryPlane	No-slip
Pressure	mapped	fixedValue	symmetryPlane	zeroGradient
Turbulent kinetic energy (k)	mapped	inletOutlet	symmetryPlane	kqRWallFunction
Turbulent energy dissipation (ε)	mapped	inletOutlet	symmetryPlane	epsilonWallFunction
υ_t	mapped	inletOutlet	symmetryPlane	nutkWallFunction
Passive scalar	uniformFixedValue	calculated	zeroGradient	zeroGradient

3. Model verification

The numerical model is validated by comparing the results of numerical tracer simulations to the data from physical modelling measurements of Khan et al. [48]. Mesh dependency study and sensitivity analysis were carried out to choose optimum meshing density to enable both numerical accuracy and minimizing the computational costs. Mesh independency analysis was conducted with four grids of 0.950, 1.120, 1.275 and 1.346 million elements (Mesh 1, Mesh 2, Mesh 3 and Mesh 4, respectively), using hexahedron meshing technique. For each meshing configuration, the normalized numerical concentration profile at the outlet boundaries of the computational domain were compared to the physical modelling measurements of Khan et al. [48].

The model was implemented in three-dimensional Cartesian coordinate system using structured meshing technique. Accurate calculation of the flow characteristics near the

310 walls, where shear stresses are high, is vital and complicated. Therefore, to achieve high
311 accuracy in simulations near the WSP's walls, cut-cell method technique with surface
312 refinement was adopted (Figure 3).

313

314 The residence time distribution (RTD) curves are determined from the numerical
315 simulations with Mesh 1-4. Figure 4 compares the results of numerical RTD curves with
316 physical modelling tracer measurements. The physical modelling data used for validation
317 of the numerical model is only considering the isolated effects of hydraulics parameters
318 and it must be noted that results from real-life WSPs will deviate from the laboratory-
319 scale tests due to the combined effects of climate, hydrology, and ecological features. The
320 Figure highlights that numerical model is capable of approximating measurements from
321 physical model with high precision. Although the overall trend of numerical results is
322 following the measurements, small deviation from the physical modelling can be
323 observed within $0.5 < t/t_n < 0.8$.

324

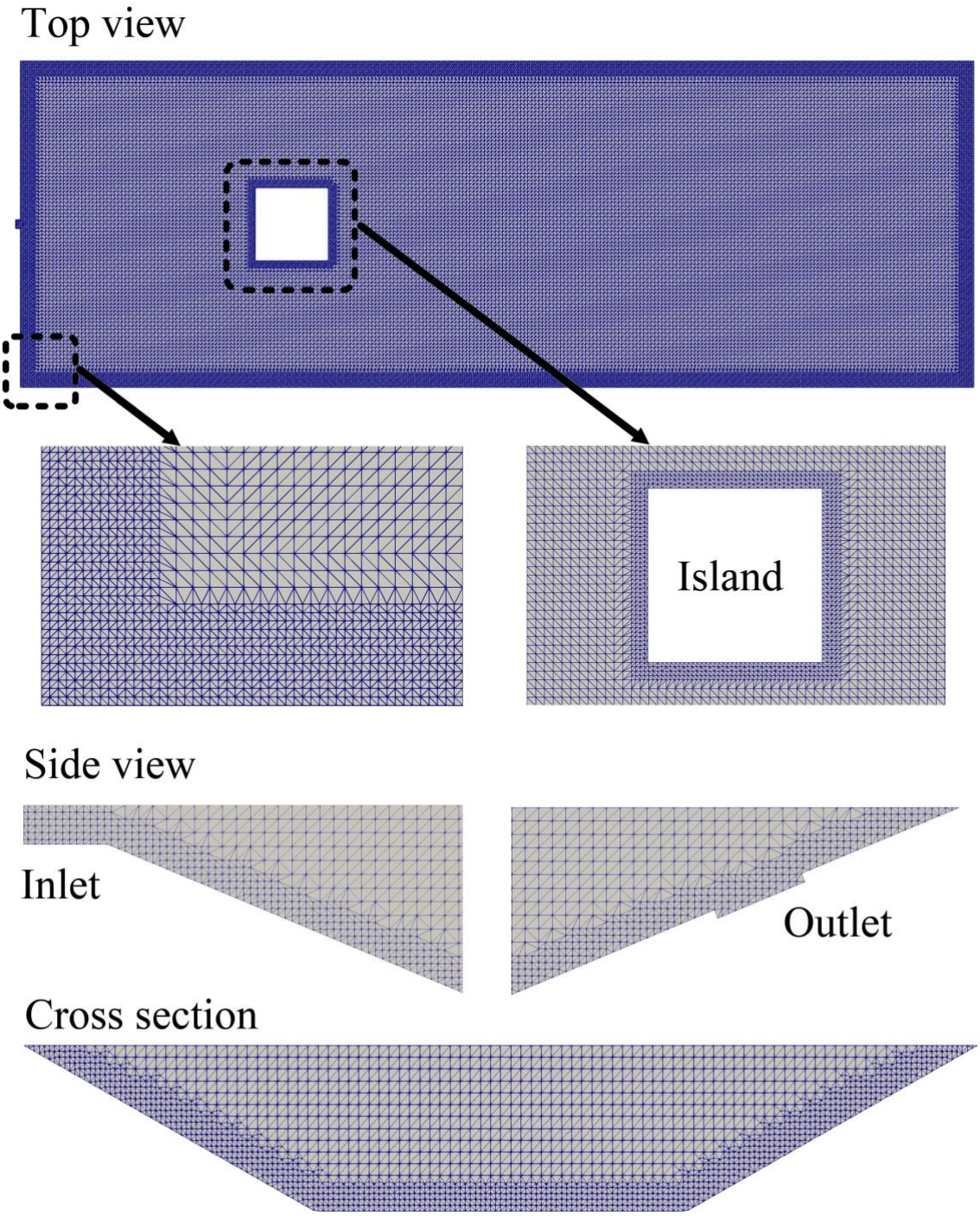

325

326 Figure 3- Numerical mesh refinement of the WSP for Mesh 3

327

328 The sensitivity analysis indicates that Mesh 3 provides the best trades-off between

329 numerical accuracy and computational costs. Hence, 1.275 million elements (Mesh 3)

using structured hexahedron mesh were generated to develop numerical domain of the WSP and conduct numerical investigations for the test cases summarized in Table 2.

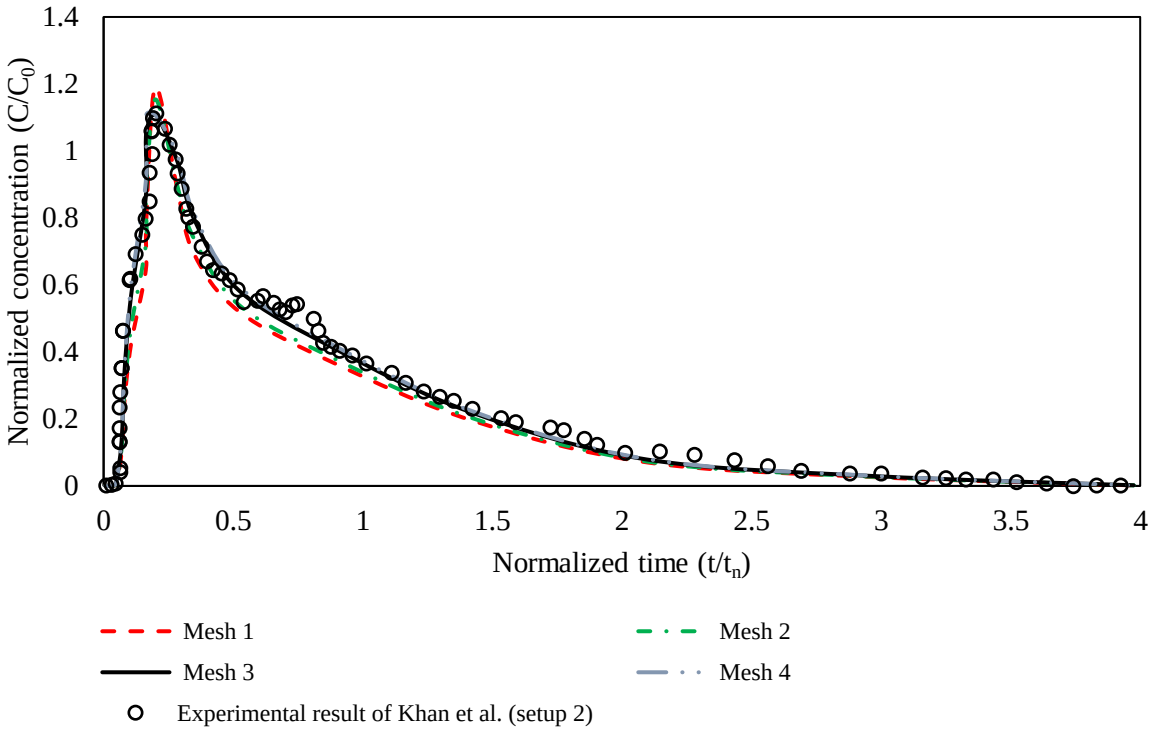

Figure 4 - Comparison of normalized RTD curves from the numerical simulations (Mesh 1 – 4) with the physical modelling measurements of Khan et al. [48]

4. Results and Discussion

Following successful validation and calibration of the numerical model (§3.), the modelling scenarios described in Table 2 are computed to investigate the effects of island orientations and side-walls slope on the hydraulic efficiency of the waste stabilization pond. The hydrodynamic and tracer simulation results for the fifteen configurations tested in this study are analyzed and elaborated with the view of understanding the impacts of

343 impervious obstacle orientation and side-walls slope on the underlying flow transport
344 patterns and solute mixing in the WSP.

345

346 Flow hydrodynamics is simulated for more than four times of the WSP's nominal
347 hydraulic retention time in order to reach steady-state flow condition. The tracer is
348 injected at the numerical inlet after reaching the steady-state condition. The numerical
349 RTD curves are determined by computing temporal evolution of tracer concentration at
350 the outlet boundary. The hydraulic characteristics of the WSPs with different island and
351 side-walls slope configurations are computed to evaluate performance of the pond under
352 different design settings.

353

354 Figures 5 – 7 show temporal evolution of normalized RTD profiles determined based on
355 tracer transport and mixing across the WSP for all the test cases investigated in this paper.
356 The RTD curves are generated based on the first 2500 seconds of the tracer simulations
357 to provide a better perspective of when the outflow concentration reaches the background
358 concentration. The RTD curves illustrate the transport and mixing of the tracer in the
359 WSP, representing the real time that water resides in the WSP. The real hydraulic
360 retention time (HRT_R) and short-circuiting are the most important parameters for
361 determining the treatment efficiency of the WSP. The efficiency of the pollutant removal
362 processes in the WSP will be adversely affected if the fluid volume passes through the
363 WSP is faster than the designed retention time.

364

Figure 5 highlights the effects of side-walls slopes on mixing and transport of tracer in absence of island. For the case of NI_2-1 and NI_1.5-1, two sharp peaks in the RTD curves are observed. The first peak in the RTD curve happens very quickly and corresponds to the time that the main core of tracer mass leaves the WSP due to short-circuiting. The second concentration peak takes place when the remaining tracer circulates across the WSP and reach the outlet boundary. The trend of temporal variations of the concentration profiles for NI_2-1 and NI_1.5-1, demonstrate a rapid increase of RTD curves immediately after the tracer introduced to the WSP, indicating undesirable short-circuiting condition (= 0.127 and 0.129, respectively) in the WSP. For NI_2-1 and NI_1.5-1 cases, concentration of the tracer at the outlet boundary reaches the maximum level after ~ 2.20 and 3.17 minutes, respectively, and the ratio of the peak time (T_{peak}) to the nominal residence time (HRT_N) is determined as 18.2% (NI_2-1) and 22.5% (NI_1.5-1), indicating inefficiency in the hydraulic performance of the WSP for these configurations with mild side-walls slope and no island. The comparison of tracer concentrations in Figure 5 shows that T_{peak} for cases NI_1-1, NI_0.5-1 and NI_0-1 is increased, respectively, while the peak of tracer concentration at the outlet is decreased for these cases. The short-circuiting values determined for the cases NI_1-1, NI_0.5-1 and NI_0-1 are increased, which highlight improvement in WSP's hydraulic efficiency (see Table 4).

The findings for the cases of WSP with no island are in line with the well-established physical modelling and field-based studies [33, 58]. Further in-depth details of the hydraulic efficiency indexes are determined and summarized in Table 4. Comparison of the RTD curves for the cases of WSP with no island shows that hydraulic efficiency and

short-circuiting condition of the WSP are improved by increase in side-walls slope, while effective volume is decreased. It was shown that changing side-walls slope from 2-1 to 0-1 increases the volume of the dead zones (i.e. reduction in effective volume) in the corner of the WSP, which is evidenced by longer tail of RTD curves in Figure 5.

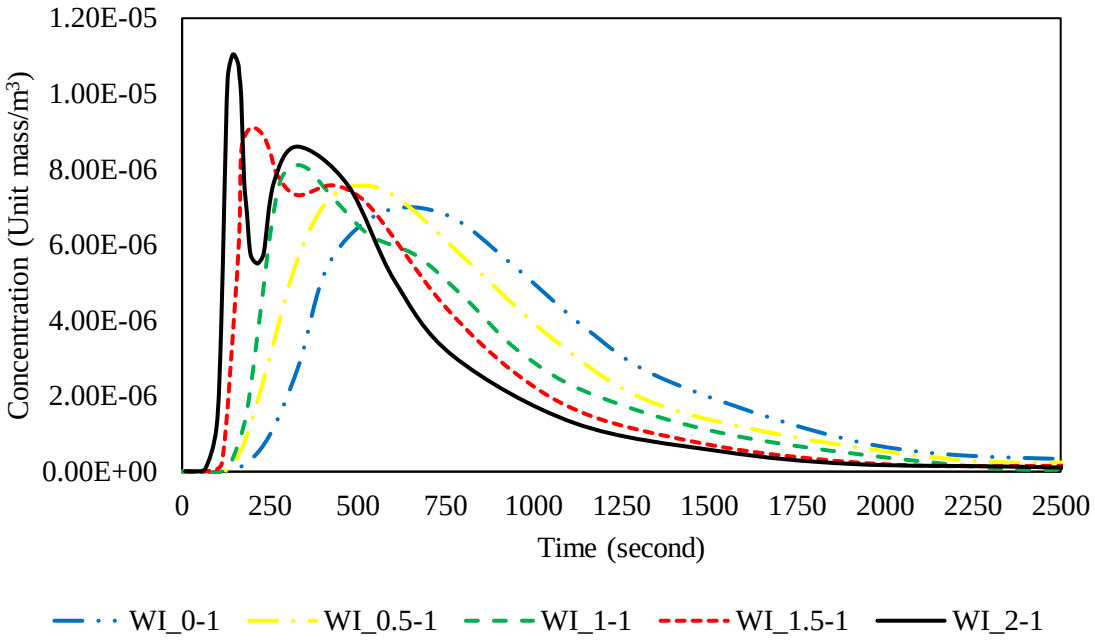

Figure 5 - RTD curves for the cases of WSPs without island

Previous studies show that hydraulic performance of treatment ponds and their retention time can get enhanced by implementing retrofitting structures such as island and baffle [17, 59]. This study investigates the combined effects of island configurations and side-walls slope on the hydraulic efficiency of WSPs, using the numerical model developed in sections §2.1 and §2.2. Figures 6 and 7 show the RTD curves determined from tracer simulations of WSP with parallel island and rotated island with a range of side-walls slopes, respectively.

For the simulation cases with mild side slopes of 2:1 and 1.5:1, it was found that for both parallel and rotated island configurations, the T_{peak} of tracer distribution at the outlet boundary was reduced indicating a significant reduction in short-circuiting condition across the WSP in comparison to the no island configurations. The results show that the implementation of an island in front of the inlet, directs the inflow jet towards the side-walls of the WSP and increases the length of flow path across the WSP from the inlet to the outlet (Figures 6 and 10). Increase in side-walls slope was shown to have positive impact on short-circuiting condition across the pond and improved the hydraulic efficiency for the cases PI_1-1, PI_0.5-1 and PI_0-1. Increase of side-walls slope for WSPs with parallel island resulted in an increased reside time of tracer in the pond which is directly associated with the longer stream path across the path from the inlet to the outlet of the pond (Figures 6 and 10, Table 4). The longer tail of RTD curves as well as lower concentration peak for cases PI_1-1, PI_0.5-1 and PI_0-1 indicate improvement in mixing and dilution across the pond.

The hydraulic efficiency of the WSP was decreased for PI_2-1 and PI_1.5-1 by about 2.9 and 3.2 percent, in comparison with NI_2-1 and NI_1.5-1. However, for the cases of WSPs with side-walls slope of 1:1, 0.5:1 and 0:1, implementation of parallel island has improved the hydraulic efficiency of the WSP by 2.5, 3.1 and 4.5 percent, respectively.

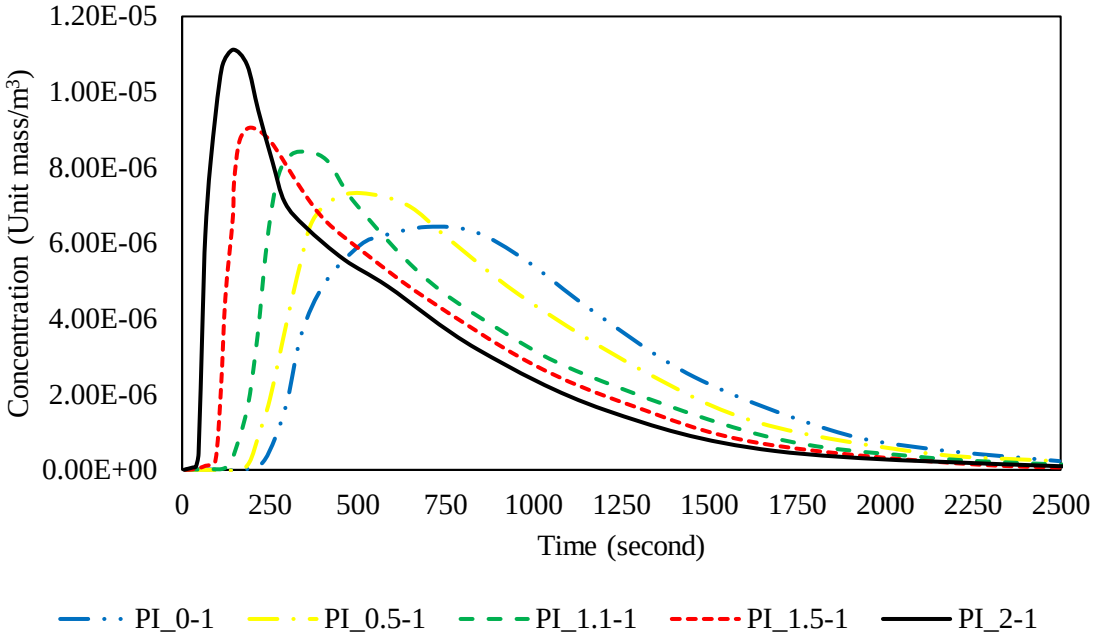

Figure 6 - RTD curves for the cases of WSPs with parallel island

This study also computed and analyzed the effects of implementing a rotated island in WSPs with a range of different side-walls slopes. The hydraulic efficiency indexes were computed for all the simulation scenarios with rotated island (see Table 4). The temporal variation of numerical tracer concentration profiles at the outlet boundary of the WSP with a rotated island and varying side-walls slope are presented in Figure 7. The sharp rise in the RTD curves for RI_2-1 and RI_1.5-1, just after the tracer was introduced in the numerical domain, indicates poor mixing condition in the WSP due to inappropriate flow conditions and short circuiting, in comparison with the cases with similar side-walls slope without island and with parallel island. Short circuiting condition is improved with the increase in the side-walls slope for RI_1-1, RI_0.5-1 and RI_0-1 cases, as the rotated island hindered inflow jet, although hydraulic efficiency indexes were not further improved for the rotated island due to reduction in HRT_R.

Hydraulic characteristics of all the simulation cases are determined based on temporally averaged integration of tracer concentration at the outlet of the WSP. Short-circuiting and hydraulic efficiency of the WSPs were improved by increasing the side-walls slope across all simulation scenarios. The effective volume of the WSPs was reduced by increasing the side-walls slope. The reduction in effective volume of the WSP was associated with the formation of dead zones in the corners of the WSP for cases with side-walls slope of 0.5:1 and 0:1.

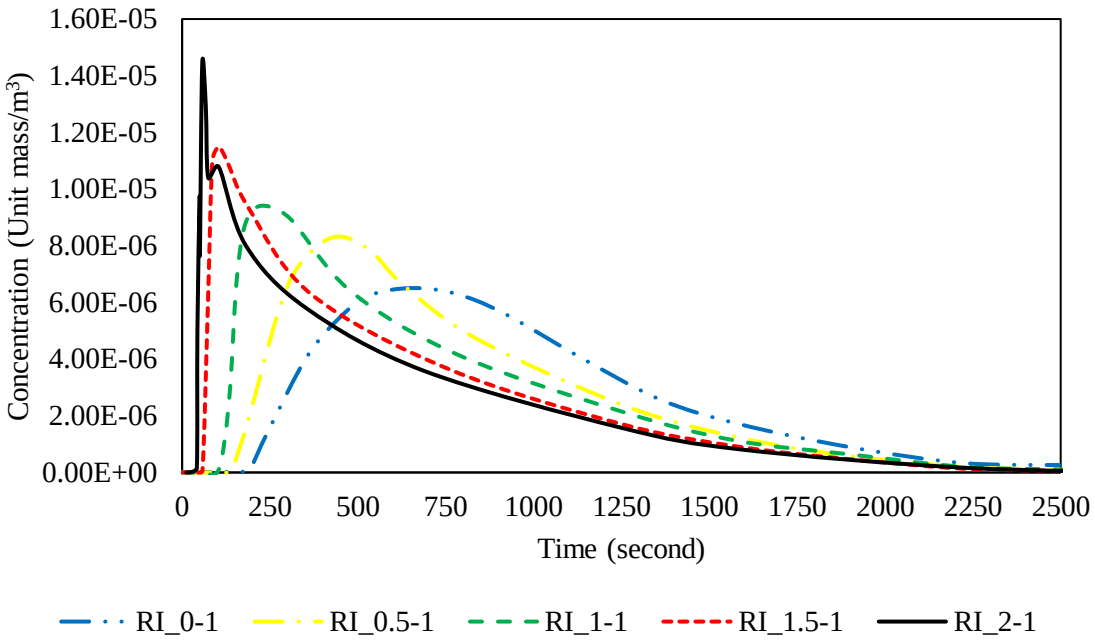

Figure 7 - RTD curves for WSPs with rotated island

The detailed hydraulic analysis of the simulation results presented in Table 4 highlights the significance of geometrical design and retrofitting on the performance of the WSPs. The proposed numerical model can be used to enhance the design of WSPs and provide detailed analysis of the performance of WSPs under a range of design and operational

conditions. The numerical algorithm developed in this study will enable modelling-informed optimum design and operation of WSPs for nature-based water and wastewater treatment processes. Optimized design and operation of WSPs will improve the treatment efficiency of the pond and reduce the pollutant discharge from WSPs to the environment enhancing the ecological features within the pond and its immediate surroundings, facilitating ecosystem restoration. Hence, the scenario modelling and detailed hydraulic analysis (Table 4) facilitates improving the environmental safety of WSPs as a nature-based solution, protecting, and enhancing the ecosystem within the WSPs as well as their surrounding environment.

Table 4 – Hydraulic characteristics of WSP for all the simulation scenarios

Case	HRT_R (min)	T_{peak} (min)	HRT_N (min)	e (%)	Short-circuiting	Hydraulic efficiency (%)
NI_2-1	11.8	2.20	12.1	97	0.127	18.2
NI_1.5-1	13.51	3.17	14.1	95.8	0.129	22.5
NI_1-1	14.8	5.57	15.79	93.7	0.141	35.3
NI_0.5-1	15.99	8.00	17.59	90.9	0.159	45.5
NI_0-1	16.86	11.00	19.47	86.6	0.173	56.5
PI_2-1	11.2	1.80	11.8	95	0.067	15.3
PI_1.5-1	12.7	2.60	13.48	94.2	0.127	19.3
PI_1-1	14.14	5.75	15.17	93.2	0.159	37.9
PI_0.5-1	15.56	8.25	16.97	91.7	0.204	48.6
PI_0-1	16.89	11.50	18.85	89.6	0.239	61
RI_2-1	10.8	1.20	11.8	92	0.062	10.2
RI_1.5-1	12.31	2.13	13.48	91.3	0.108	15.8
RI_1-1	13.71	4.75	15.17	90.4	0.187	31.3
RI_0.5-1	15.11	7.17	16.97	89.05	0.216	42.2
RI_0-1	16.41	10.58	18.85	87.05	0.269	56.1

4.1. Hydrodynamics Analysis

Alteration in geometrical properties of WSPs can significantly influence flow hydrodynamics patterns across the pond, and consequently change the efficiency of treatment processes. Therefore, detailed understanding of the effects of geometrical designs and retrofitting structures on flow hydrodynamics and solute transport across the WSPs is key for optimized design, operations, and maintenance of treatment ponds. Detailed flow hydrodynamics properties are determined for the simulation cases outlined in Table 2, to investigate the impacts of geometrical properties on the flow and solute transport across WSPs and quantify the effectiveness of WSPs. Figure 8 compares the lateral flow velocity profiles across the width of the WSPs for the simulation scenarios with parallel and rotated island.

Understanding the velocity profiles across the WSP is key for improvement of hydraulic efficiency, sludge management and control of biological treatment processes in treatment ponds [20, 21, 60]. The averaged lateral numerical velocity profiles are determined in the middle of the WSP which is of importance for reducing short circuiting conditions. Analysis of the results shows that retrofitting of island has led to creation of shear velocity profiles across the width of the WSP. Water inflow from the inlet is divided into two distinct flow regimes, where near the sides of the WSP flow is advecting towards the outlet with a positive velocity and as moving from the side-walls, the flow velocity decrease until it reaches the minimum velocity at the center of the pond. The positive velocity values in Figure 8 indicate flow direction towards the outlet and the negative velocities show flow movement towards the inlet.

The variation of the lateral flow velocity profiles in WSP for both parallel and rotated island with the side-walls slope of 2:1 and 1.5:1 is significant, ranging from -0.02 to 0.1(m/s). Analysis of the results presented in Figure 8 show that parallel island performs better in reducing the inflow jet velocity and improvement of flow short circuiting condition across the WSP, in comparison to the results obtained for cases with rotated island. For all the tested configurations, it was shown that the maximum lateral velocities in both directions are greater for the WSPs with rotated island.

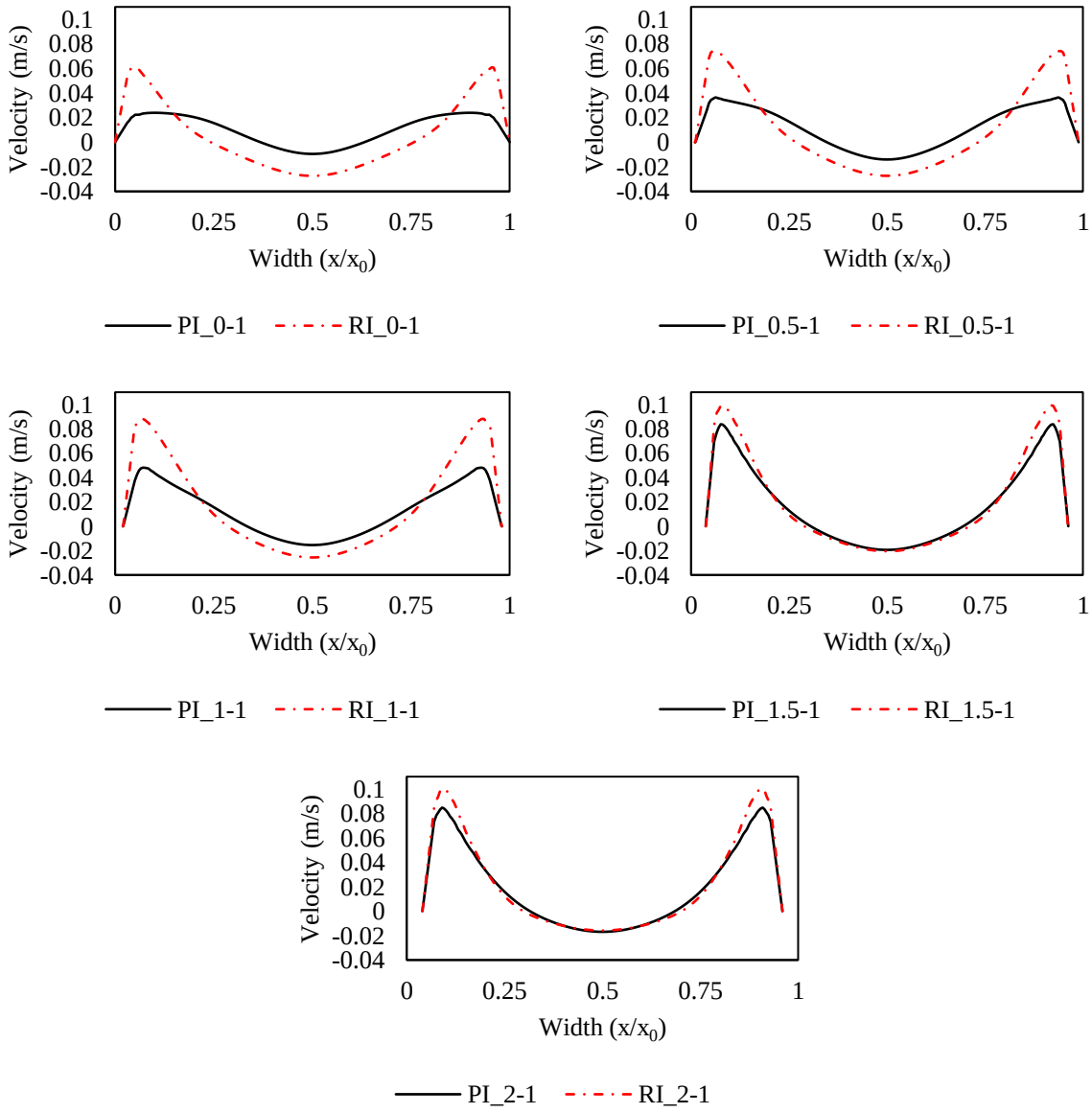

Figure 8 - Lateral velocity profiles for WSPs of varying wall-slope in presence of parallel and rotated island

498

499 The vertical variations of flow velocity profiles are determined for all the simulation
500 scenarios. Figure 9 illustrates the variation of the velocity profiles over the depth of the
501 WSPs, determined at the middle of the pond and after the island retrofitting. The negative
502 velocity values in Figure 9 highlights reverse flow direction (i.e. towards the inlet) and
503 positive velocities indicate flow direction towards the outlet boundaries. The analysis of

numerical results show that the vertical flow velocity profiles were increased as the side-walls slope was reduced. The vertical velocity profiles for ponds with rotated island were greater in comparison to those configurations with parallel island.

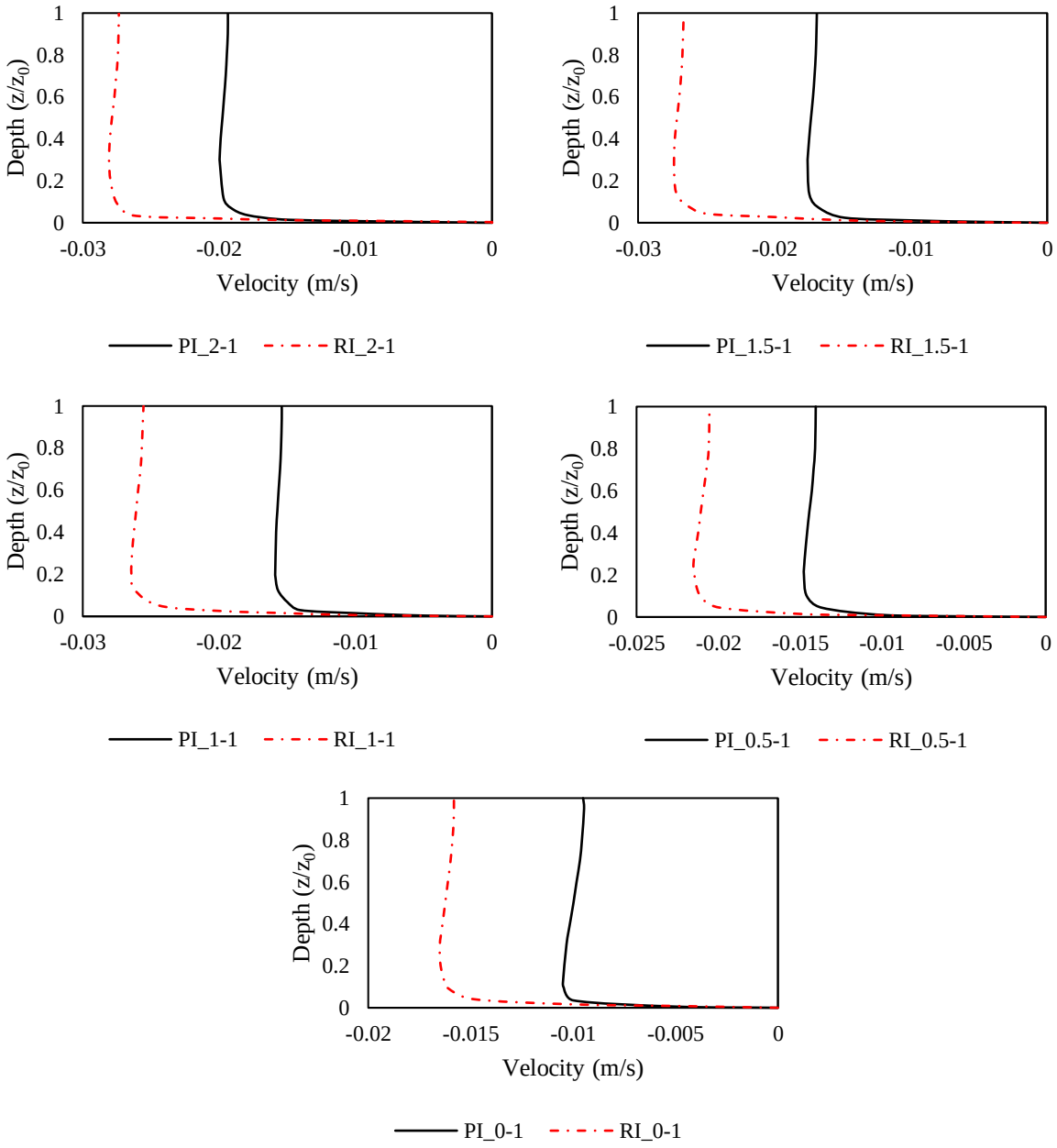

Figure 9 -Vertical velocity profiles for WSPs with parallel and rotated island

509 The effects of island configurations and side-walls slopes are further investigated through
510 determining the solute tracer flow path and streamlines across the pond. Figures 10 and
511 11 show flow streamlines computed for all the simulation cases with parallel and rotated
512 island. Four main circulation zones can be seen in the pond across all the test cases. Two
513 distinct circulation zones of similar length are evident before the islands for all the cases
514 presented in Figure 10 and 11. For the cases with milder side-walls slope (e.g., PI 2-1 and
515 RI 2-1) additional smaller size dead zones are generated in the corners of the WSP near
516 the inlet. Analysis of solute streamlines across the pond highlights that island
517 configurations and side-walls slope are playing significant role in forming the circulation
518 patterns and structure of dead zones after the retrofitting island, which determine the
519 hydraulic performance of the WSP. Detailed understanding of flow path across the WSP
520 and analysis of re-circulation zones facilitated through scenario modelling using the
521 numerical model developed in this study is important for assessing the performance of
522 WSP and their impacts on the ecological function of the pond and its surroundings.
523

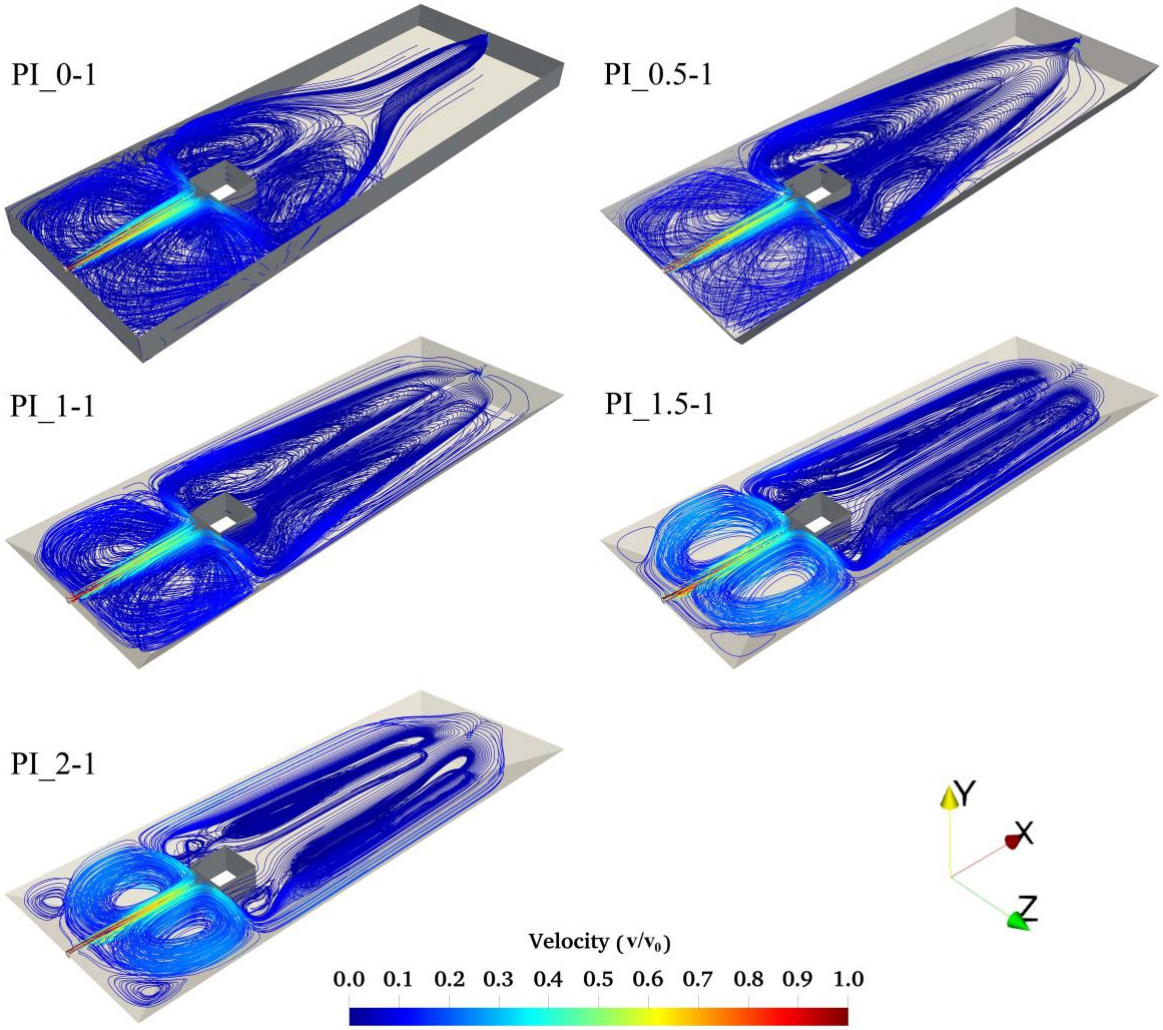

Figure 10 – Flow transport path (streamlines) for the cases of WSP with parallel island

The spatial distribution of flow turbulent kinetic energy across the WSP was determined for all the simulation scenarios to provide a better understanding of impacts of geometrical configurations on solute transport and mixing. Figures 12 and 13 depict the effects of geometrical properties on the distributions of turbulent kinematic energy (k) across the WSP with parallel and rotated island retrofitting. The normalized non-dimensional turbulent kinetic energy is defined as the ratio of k/k_0. The results indicate

that island installation, in general, led to abrupt dissipation of inflow kinetic energy and improved the treatment performance of WSPs.

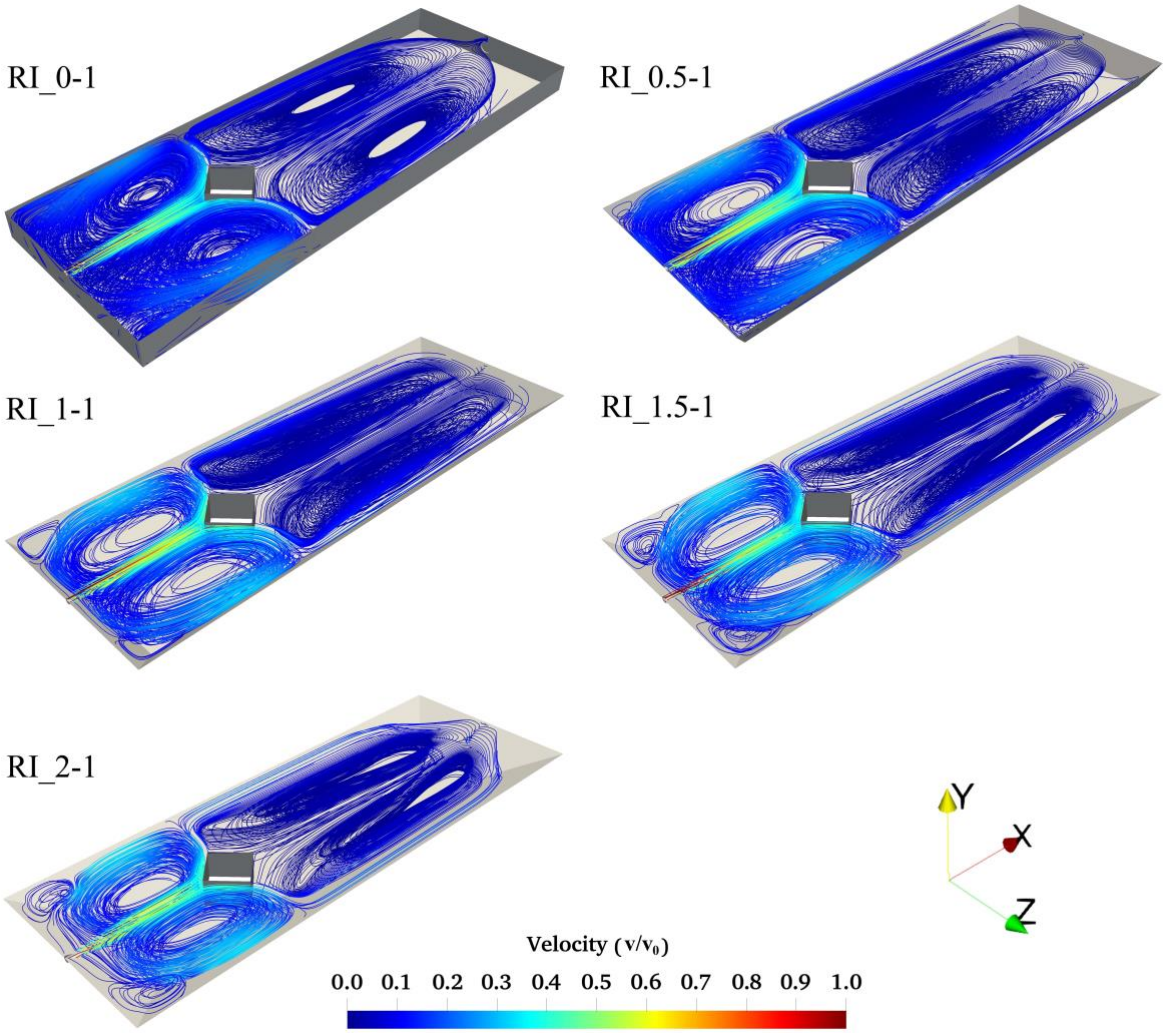

Figure 11 – Flow transport path (streamlines) for the cases of WSP with rotated island

Reduction of inflow turbulent kinematic energy for the cases with parallel retrofitting island is more apparent compared to the rotated island, indicating in better dilution and mixing regime in the WSP with parallel island retrofitting. The turbulent kinetic energy

values behind the island and near the walls for the cases with rotated island is slightly larger than the cases with parallel island, which led to reduced hydraulic performance and short circuiting for simulation scenarios with rotated island retrofitting. Development of turbulent kinetic energy behind the island for both rotated and parallel cases is increased as the side-walls slope changed from 0:1 to 2:1.

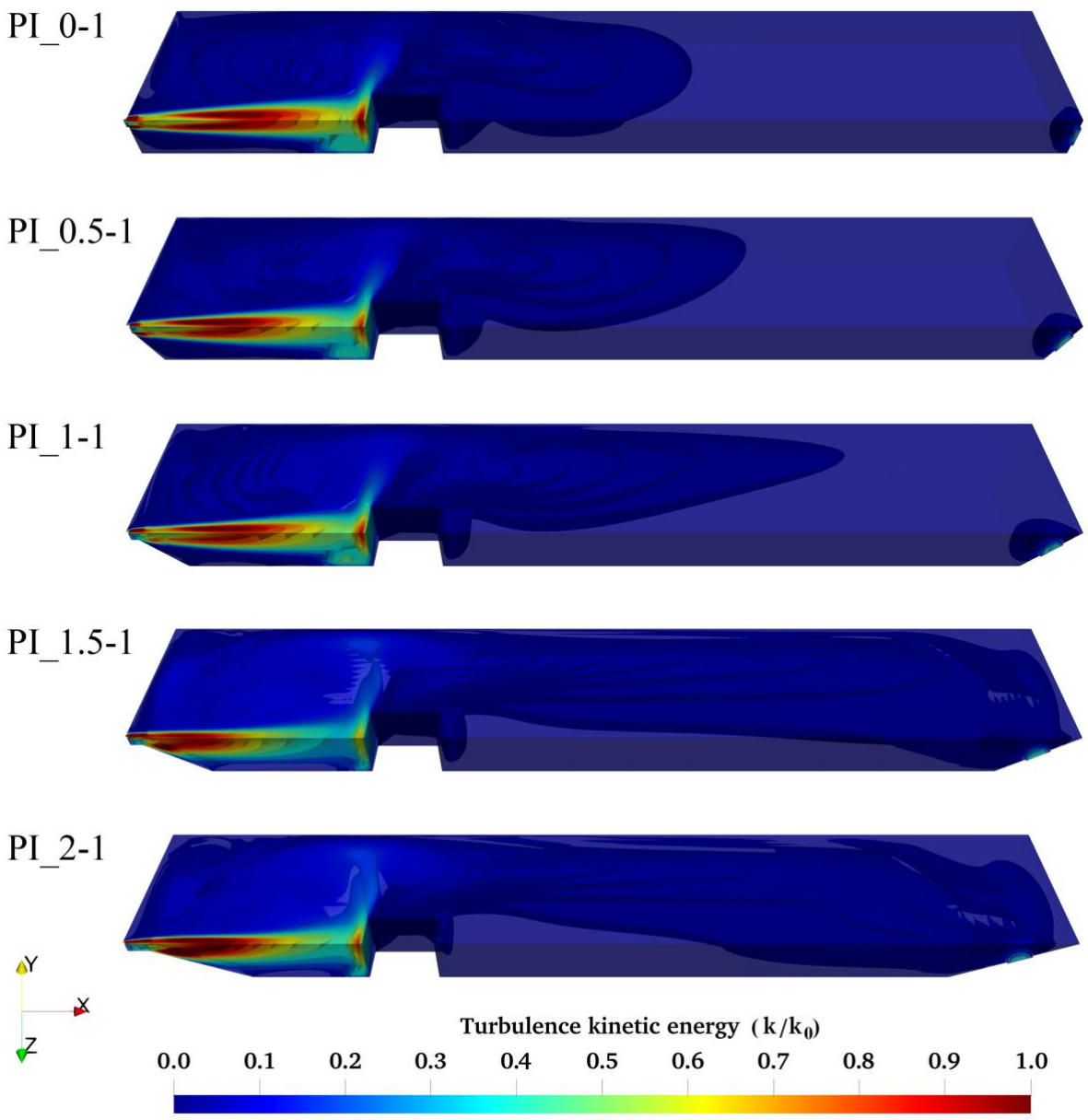

548

549 Figure 12 – Spatial variation of non-dimensionalized turbulent kinetic energy (k/k_0) across the
550 WSPs with parallel island

551

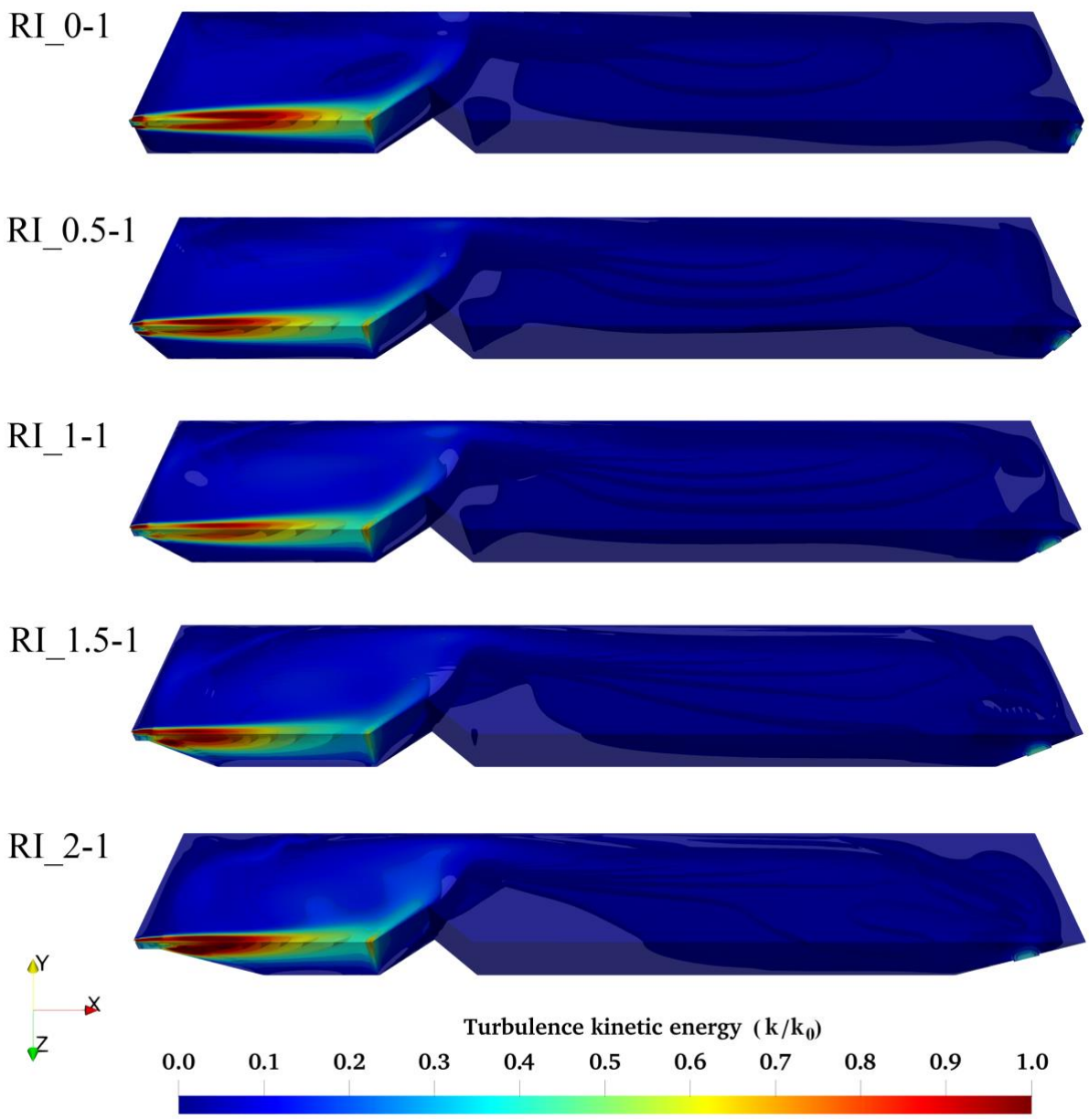

552

553 Figure 13 – Spatial variation of non-dimensionalized turbulent kinetic energy (k/k_0) across the
554 WSPs with rotated island

555

556 Lateral turbulent kinetic energy profiles for the test configurations with parallel and
557 rotated island are determined and shown in Figure 14. The results show increase of
558 turbulent kinetic energy near the walls as the island directed water flow towards the sides.

559 It can be inferred that parallel island has better performance in reduction of inflow
560 turbulent kinetic energy. Analysis of the results also show that side-walls slope directly
561 influences the distribution of turbulent kinetic energy and consequently the solute
562 residence time in the WSP. Figure 14 shows that the inflow turbulent kinematic energy is
563 more dampened for the cases with steeper side-walls slope.

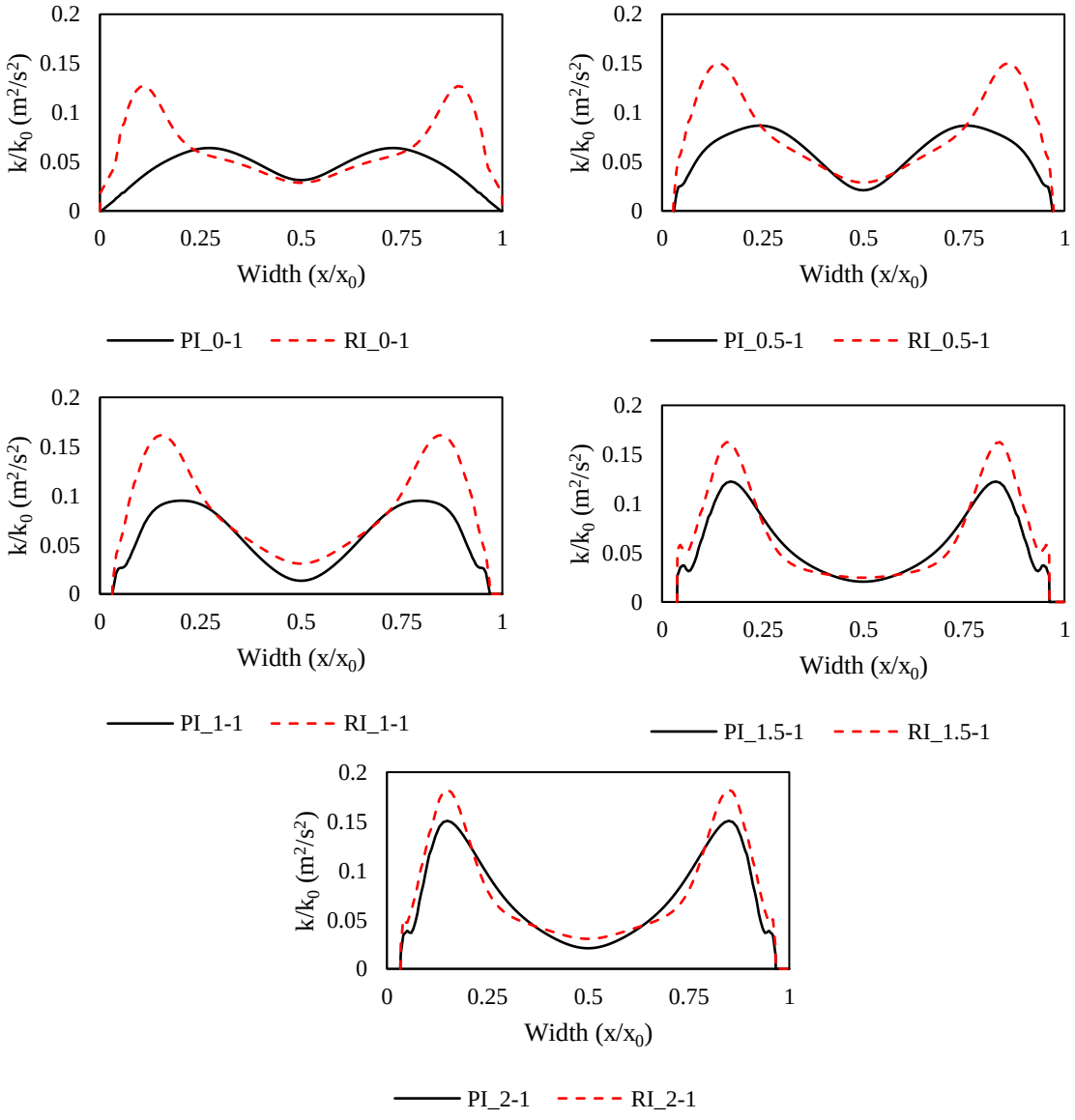

Figure 14 – Lateral turbulent kinematic energy profiles for the cases of WSPs with parallel and rotated island

564

5. Conclusions

Hydraulics characteristics and solute transport processes in a waste stabilization pond (WSP) is investigated in this paper. A hydrodynamic model is developed using RANS equations with *k-ε* turbulence closure model. Solute transport was simulated by coupling the advection-diffusion model with the hydrodynamic model. The proposed model was successfully validated and calibrated against physical modelling measurements of Khan et al. [48]. Fifteen simulation scenarios were designed to provide a comprehensive analysis of the effects of waste stabilization pond's geometrical properties (i.e. side-walls slope) and island retrofitting configurations on the hydraulic efficiency and pollution transport across the pond.

Detailed hydraulics performance indexes including HRT_R, T_{peak}, HRT_N, e, Short-circuiting and Hydraulic efficiency were determined for all simulation cases. The analysis of the simulation results show that increase in the side-walls slope and implementation of island enhanced the short circuiting and hydraulic efficiency of the pond. The comparison of results between parallel and rotated island retrofitting show that parallel island configurations provide better hydraulic efficiency and improve the short-circuiting conditions across the pond.

Vertical and lateral velocity profiles across the ponds were determined to investigate the effects of side-walls slope and island retrofitting on the hydraulic and treatment efficiency of the pond. Lateral velocity profiles show presence of strong shear velocity profile due to island retrofitting which enhanced the mixing and treatment efficiency of the pond.

588 Non-reactive passive tracer transport across the waste stabilization pond (WSP) was
589 determined for all the simulation scenarios, to investigate solute interactions with the
590 WSP and the effects of geometrical configurations on the formation of dead zones across
591 the pond. Further analysis was conducted to determine turbulent kinetic energy profiles
592 for simulation scenarios. It was shown that parallel island retrofitting has better
593 performance in reducing the flow kinetic energy and increasing the solute residence time
594 in the WSP, leading to enhanced treatment efficiency.

595

596 The numerical results indicate that even minimal alterations to geometrical properties can
597 significantly affect the hydraulic performance and treatment efficiency of the WSP.
598 Hence, careful considerations are needed to investigate the hydraulic characteristics of
599 treatment ponds for different design and operational conditions. It was shown that the
600 numerical model developed within this study is capable of robust simulation of
601 hydrodynamics and solute transport for waste stabilization ponds. Detailed understanding
602 of flow and tracer transport from the developed model enabled identification and
603 quantification of key performance indicators of the waste stabilization ponds. Given that
604 in practical settings multiple connected ponds are adopted, further physical modelling
605 measurements are required to validate and fine-tune the proposed model for multiple
606 WSPs system.

607 The proposed model can help identify appropriate design configurations of treatment
608 ponds to enhance treatment efficiency and reduce operational costs. Modelling-informed
609 optimum design and operation of WSPs for nature-based water and wastewater treatment
610 processes is vital to ensure pollution loading from WSPs to the environment is minimized,

and the ecological features within the pond and its immediate surroundings are protected. As such, adoption of the proposed numerical tool for scenario modelling and detailed hydraulic analysis facilitates improving the environmental safety of WSPs.

References

[1] D.J. Rodriguez, C. Van den Berg, A. McMahon, Investing in water infrastructure: capital, operations and maintenance, (2012).

[2] A. Alighardashi, D. Goodarzi, Simulation of depth and wind effects on the hydraulic efficiency of sedimentation tanks, Water and Environment Journal. ttps://doi.org/10.1111/wej.12478.

[3] D. Goodarzi, S. Abolfathi, S. Borzooei, Modelling solute transport in water disinfection systems: Effects of temperature gradient on the hydraulic and disinfection efficiency of serpentine chlorine contact tanks, Journal of Water Process Engineering. 37 (2020) 101411. https://doi.org/10.1016/j.jwpe.2020.101411.

[4] S. Borzooei, G.H.B. Miranda, S. Abolfathi, G. Scibilia, L. Meucci, M.C. Zanetti, Application of unsupervised learning and process simulation for energy optimization of a WWTP under various weather conditions, Water Science and Technology. 81 (8) (2020) 1541-1551. 10.2166/wst.2020.220.

[5] S. Borzooei, Y. Amerlinck, D. Panepinto, S. Abolfathi, I. Nopens, G. Scibilia, L. Meucci, M.C. Zanetti, Energy optimization of a wastewater treatment plant based on energy audit data: small investment with high return, Environmental Science

633 and Pollution Research. 27 (15) (2020) 17972-17985. 10.1007/s11356-020-
634 08277-3.
635 [6] S. Borzooei, R. Teegavarapu, S. Abolfathi, Y. Amerlinck, I. Nopens, M.C.
636 Zanetti, Data Mining Application in Assessment of Weather-Based Influent
637 Scenarios for a WWTP: Getting the Most Out of Plant Historical Data, Water,
638 Air, & Soil Pollution. 230 (1) (2018) 5. 10.1007/s11270-018-4053-1.
639 [7] C. Lashford, M. Rubinato, Y. Cai, J. Hou, S. Abolfathi, S. Coupe, S.
640 Charlesworth, S. Tait, SuDS & Sponge Cities: A Comparative Analysis of
641 the Implementation of Pluvial Flood Management in the UK and China,
642 Sustainability. 11 (1) (2019) 213.
643 [8] S. Borzooei, Y. Amerlinck, S. Abolfathi, D. Panepinto, I. Nopens, E. Lorenzi, L.
644 Meucci, M.C. Zanetti, Data scarcity in modelling and simulation of a large-scale
645 WWTP: Stop sign or a challenge, Journal of Water Process Engineering. 28
646 (2019) 10-20. https://doi.org/10.1016/j.jwpe.2018.12.010.
647 [9] S.B. Grant, J.-D. Saphores, D.L. Feldman, A.J. Hamilton, T.D. Fletcher, P.L.
648 Cook, M. Stewardson, B.F. Sanders, L.A. Levin, R.F. Ambrose, Taking the
649 “waste” out of “wastewater” for human water security and ecosystem
650 sustainability, science. 337 (6095) (2012) 681-686. 10.1126/science.1216852.
651 [10] J.G. Hering, T.D. Waite, R.G. Luthy, J.E. Drewes, D.L. Sedlak, *A changing*
652 *framework for urban water systems*. 2013, ACS Publications.
653 [11] D. Goodarzi, K.S. Lari, A. Alighardashi, A large eddy simulation study to assess
654 low-speed wind and baffle orientation effects in a water treatment sedimentation

655 basin, Water Science and Technology. 2017 (2) (2018) 412-421.
656 https://doi.org/10.2166/wst.2018.171.
657 [12] F.R. Spellman, J.E. Drinan. Wastewater stabilization ponds, CRC Press, 2014.
658 [13] G.Z. Watters, The hydraulics of waste stabilization ponds. Utah Water Research
659 Laboratory, Logan., (1972).
660 [14] M.E. Verbyla, J.R. Mihelcic, A review of virus removal in wastewater treatment
661 pond systems, Water research. 71 (2015) 107-124.
662 https://doi.org/10.1016/j.watres.2014.12.031.
663 [15] M.E. Verbyla, S.M. Oakley, L.A. Lizima, J. Zhang, M. Iriarte, A.E. Tejada-
664 Martinez, J.R. Mihelcic, Taenia eggs in a stabilization pond system with poor
665 hydraulics: concern for human cysticercosis?, Water Science and Technology. 68
666 (12) (2013) 2698-2703. https://doi.org/10.2166/wst.2013.556.
667 [16] C. Banda, P. Sleigh, D. Mara. *3D-CFD modelling of E. coli removal in baffled*
668 *primary facultative ponds: classical design optimization*. in *IWA specialist*
669 *conference on waste stabilization ponds, Bangkok, Thailand*. 2006.
670 [17] J. Persson, The hydraulic performance of ponds of various layouts, Urban Water.
671 2 (3) (2000) 243-250. https://doi.org/10.1016/S1462-0758(00)00059-5.
672 [18] D. Sweeney, J. Nixon, N.J. Cromar, H.J. Fallowfield, Profiling and modelling of
673 thermal changes in a large waste stabilisation pond, Water Science and
674 Technology. 51 (12) (2005) 163-172. https://doi.org/10.2166/wst.2005.0454.
675 [19] J.C. Crittenden, R.R. Trussell, D.W. Hand, K.J. Howe, G. Tchobanoglous.
676 MWH's water treatment: principles and design, John Wiley & Sons, 2012.

[20] F.R. Ouedraogo, J. Zhang, P.K. Cornejo, Q. Zhang, J.R. Mihelcic, A.E. Tejada-Martinez, Impact of sludge layer geometry on the hydraulic performance of a waste stabilization pond, Water research. 99 (2016) 253-262. https://doi.org/10.1016/j.watres.2016.05.011.

[21] L.X. Coggins, M. Ghisalberti, A. Ghadouani, Sludge accumulation and distribution impact the hydraulic performance in waste stabilisation ponds, Water Research. 110 (2017) 354-365. https://doi.org/10.1016/j.watres.2016.11.031.

[22] A. Alvarado, E. Sanchez, G. Durazno, M. Vesvikar, I. Nopens, CFD analysis of sludge accumulation and hydraulic performance of a waste stabilization pond, Water Science and Technology. 66 (11) (2012) 2370-2377. https://doi.org/10.2166/wst.2012.450.

[23] A. Alvarado, S. Vedantam, G. Durazno, I. Nopens, Hydraulic assessment of waste stabilization ponds: Comparison of computational fluid dynamics simulations against tracer data, Maskana. 2 (1) (2011) 81-89. https://doi.org/10.18537/mskn.02.01.05.

[24] A. Broughton, A. Shilton, Tracer studies on an aerated lagoon, Water Science and Technology. 65 (4) (2012) 611-617. https://doi.org/10.2166/wst.2012.906.

[25] M. Short, N. Cromar, H. Fallowfield, Hydrodynamic performance of pilot-scale duckweed, algal-based, rock filter and attached-growth media reactors used for waste stabilisation pond research, Ecological Engineering. 36 (12) (2010) 1700-1708. https://doi.org/10.1016/j.ecoleng.2010.07.015https://doi.org/10.1016/j.ecoleng.2010.07.015.

[26] P. Barter, Investigation of pond velocities using dye and small drogues: a case study of the Nelson City waste stabilisation pond, Water science and technology. 48 (2) (2003) 145-151. https://doi.org/10.2166/wst.2003.0107.

[27] J. Fyfe, J. Smalley, D. Hagare, M. Sivakumar, Physical and hydrodynamic characteristics of a dairy shed waste stabilisation pond system, Water science and technology. 55 (11) (2007) 11-20. https://doi.org/10.2166/wst.2007.337.

[28] A. Shilton, M. Kerr. *Field measurements of in-pond velocities by a drogue and survey technique*. in *Proceedings of the 4th IAWQ Specialist Group Conference on Waste Stabilisation Ponds, Marrakech, Morocco*. 1999.

[29] R.P. Canale, M.T. Auer, E.M. Owens, T.M. Heidtke, S.W. Effler, Modeling fecal coliform bacteria—II. Model development and application, Water Research. 27 (4) (1993) 703-714. https://doi.org/10.1016/0043-1354(93)90180-P.

[30] R.A. Ferrara, D.R. Harleman, Hydraulic modeling for waste stabilization ponds, Journal of the Environmental Engineering Division. 107 (4) (1981) 817-830.

[31] A.W. Mayo, Modeling coliform mortality in waste stabilization ponds, Journal of Environmental Engineering. 121 (2) (1995) 140-152. https://doi.org/10.1061/(ASCE)0733-9372(1995)121:2(140).

[32] C. Polprasert, K.K. Bhattarai, Dispersion model for waste stabilization ponds, Journal of environmental engineering. 111 (1) (1985) 45-59. https://doi.org/10.1061/(ASCE)0733-9372(1985)111:1(45).

[33] M. Wood, T. Howes, J. Keller, M. Johns, Two dimensional computational fluid dynamic models for waste stabilisation ponds, Water Research. 32 (3) (1998) 958-963. https://doi.org/10.1016/S0043-1354(97)00316-3.

[34] M. Wood, P. Greenfield, T. Howes, M. Johns, J. Keller, Computational fluid dynamic modelling of wastewater ponds to improve design, Water Science and Technology. 31 (12) (1995) 111. https://doi.org/10.1016/0273-1223(95)00498-C.

[35] G. Vega, M. Pena, C. Ramirez, D. Mara, Application of CFD modelling to study the hydrodynamics of various anaerobic pond configurations, Water science and technology. 48 (2) (2003) 163-171. https://doi.org/10.2166/wst.2003.0111.

[36] J. Agunwamba, Effect of the Location of the Inlet and Outlet Structures on Short-Circuiting: Experimental Investigation, Water environment research. 78 (6) (2006) 580-589. https://doi.org/10.2175/106143006X109603.

[37] A. Shilton, J.H. Harrison. Guidelines for the hydraulic design of waste stabilisation ponds, Institute of Technology and Engineering, Massey University Palmerston North, 2003.

[38] A. Shilton, *Studies into the hydraulics of waste stabilisation ponds: a thesis presented in partial fulfilment of the requirements for the degree of Doctor of Philosophy in Environmental Engineering at Massey University, Turitea Campus, Palmerston North, New Zealand*. 2001, Massey University.

[39] K. Sookhak Lari, A Note on Baffle Orientation in Long Ponds, Journal of Environmental Informatics. 21 (2) (2013). 10.3808/jei.201300240.

[40] D. Mara, Waste stabilization ponds: Past, present and future, Desalination and Water Treatment. 4 (1-3) (2009) 85-88. https://doi.org/10.5004/dwt.2009.359.

[41] H. Salter, C. Ta, S. Ouki, S. Williams, Three-dimensional computational fluid dynamic modelling of a facultative lagoon, Water Science and Technology. 42 (10-11) (2000) 335-342. https://doi.org/10.2166/wst.2000.0674.

[42] J.-N. Baléo, P. Humeau, P. Le Cloirec, Numerical and experimental hydrodynamic studies of a lagoon pilot, Water research. 35 (9) (2001) 2268-2276. https://doi.org/10.1016/S0043-1354(00)00502-9.

[43] A. Shilton, D. Mara, CFD (computational fluid dynamics) modelling of baffles for optimizing tropical waste stabilization pond systems, Water Science and Technology. 51 (12) (2005) 103-106. https://doi.org/10.2166/wst.2005.0438.

[44] G. Aldana, B. Lloyd, K. Guganesharajah, N. Bracho, The development and calibration of a physical model to assist in optimising the hydraulic performance and design of maturation ponds, Water science and technology. 51 (12) (2005) 173-181. https://doi.org/10.2166/wst.2005.0456.

[45] F.E. Dierberg, J.J. Juston, T.A. DeBusk, K. Pietro, B. Gu, Relationship between hydraulic efficiency and phosphorus removal in a submerged aquatic vegetation-dominated treatment wetland, Ecological Engineering. 25 (1) (2005) 9-23. https://doi.org/10.1016/j.ecoleng.2004.12.018.

[46] A.F. Lightbody, M.E. Avener, H.M. Nepf, Observations of short-circuiting flow paths within a free-surface wetland in Augusta, Georgia, USA, Limnology and oceanography. 53 (3) (2008) 1040-1053. https://doi.org/10.4319/lo.2008.53.3.1040.

[47] S. Khan, M. Shoaib, M.M. Khan, B.W. Melville, A.Y. Shamseldin, Hydraulic investigation of the impact of retrofitting floating treatment wetlands in retention ponds, Water Science and Technology (2019). https://doi.org/10.2166/wst.2019.397.

[48] S. Khan, B. Melville, A. Shamseldin, Retrofitting a stormwater retention pond using a deflector island, Water Science and Technology. 63 (12) (2011) 2867-2872. https://doi.org/10.2166/wst.2011.569.

[49] R.G. Passos, V.V. Ferreira, M. von Sperling, A dynamic and unified model of hydrodynamics in waste stabilization ponds, Chemical Engineering Research and Design. 144 (2019) 434-443. https://doi.org/10.1016/j.watres.2016.05.011.

[50] S.B. Pope, *Turbulent flows*. 2001, IOP Publishing.

[51] *OpenFOAM User Guide version 5, 2017. OpenCFD Ltd. http://www.openfoam.com/docs/user/.*

[52] W. Jones, B.E. Launder, The prediction of laminarization with a two-equation model of turbulence, International journal of heat and mass transfer. 15 (2) (1972) 301-314.

[53] S. Khan, B.W. Melville, A.Y. Shamseldin, C. Fischer, Investigation of flow patterns in storm water retention ponds using CFD, Journal of Environmental Engineering. 139 (1) (2012) 61-69. https://doi.org/10.1061/(ASCE)EE.1943-7870.0000540.

[54] A. Alvarado, Advanced dynamic modelling of wastewater treatment ponds.(PhD), Ghent University, Belgium (2013). http://hdl.handle.net/1854/LU-3117519.

[55] L. Metcalf, H.P. Eddy, G. Tchobanoglous. Wastewater engineering: treatment, disposal, and reuse, Vol. 4, McGraw-Hill NewYork, 1972.

[56] R.B. Bird, Transport phenomena, Appl. Mech. Rev. 55 (1) (2002) R1-R4. https://doi.org/10.1115/1.1424298.

[57] M. Van Reeuwijk, K.S. Lari, Asymptotic solutions for turbulent mass transfer augmented by a first order chemical reaction, International Journal of Heat and Mass Transfer. 55 (23-24) (2012) 6485-6490. https://doi.org/10.1016/j.ijheatmasstransfer.2012.06.048.

[58] Å. Adamsson, L. Bergdahl, S. Lyngfelt, Measurement and three-dimensional simulation of flow in a rectangular detention tank, Urban Water Journal. 2 (4) (2005) 277-287. https://doi.org/10.1080/15730620500386545.

[59] Å. Adamsson, L. Bergdahl, M. Vikström, A laboratory study of the effect of an island to extend residence time in a rectangular tank, in *Global Solutions for Urban Drainage*. 2002. p. 1-10.

[60] L.X. Coggins, J. Sounness, L. Zheng, M. Ghisalberti, A. Ghadouani, Impact of Hydrodynamic Reconfiguration with Baffles on Treatment Performance in Waste Stabilisation Ponds: A Full-Scale Experiment, Water. 10 (2) (2018). 10.3390/w10020109.